Conjugated Polymers with Carbazole, Fluorene, and Ethylene Dioxythiophene in the Main Chain and a Pendant Cyano Group: Synthesis, Photophysical, and Electrochemical Studies

Vivek Anand, Elumalai Ramachandran, Raghavachari Dhamodharan
Department of Chemistry, IIT Madras, Chennai 600036, Tamil Nadu, India
Correspondence to: R. Dhamodharan (E-mail: damo@iitm.ac.in)

Received 1 April 2016; accepted 27 April 2016; published online 00 Month 2016
DOI: 10.1002/pola.28160

ABSTRACT: Six new conjugated polymers comprising of carbazole, fluorene, and ethylene dioxythiophene (EDOT) moieties along the backbone with a pendant cyano group attached to the ethylene moiety have been designed and synthesized via Sonogashira coupling polymerization reaction. Optical and electrochemical characterizations have shown that the energy band gaps lie within the range of 2.35–2.44 eV. Additionally, the presence of carbazole and EDOT makes these polymers better hole transporting materials, which is reflected from their low oxidation potential peaks (0.55–1.11 V) in cyclic voltammograms. Furthermore, the aggregation enhanced emission (AEE) phenomenon resulted in a 2.6-fold increase in fluorescence intensity in a 90:10 THF/water mixture in comparison to pristine THF. The AEE properties were further verified by DLS (dynamic light scattering) experiment and SEM (scanning electron microscopy) studies. Polymers in solution as well as in polystyrene matrix emit in the green region (quantum yield in solution state Φ_f =41–43%) with CIE values (0.25–0.36, 0.52–0.57). Excellent thermal stability is observed for the new polymers. © 2016 Wiley Periodicals, Inc. J. Polym. Sci., Part A: Polym. Chem. **2016**, *00*, 000–000

KEYWORDS: conjugated polymers; carbazole; fluorene; ethylene dioxythiophene; Sonogashira polymerization; AEE; light-emitting diodes (LED); copolymerization; luminescence

INTRODUCTION Conducting polymers (CPs)[1(a,b)] have been applied immensely in the field of organic light emitting diodes (OLEDs),[2–4] field effect transistors (FETs),[5–7] chemical sensors,[8(a,b)] and organic photovoltaics (OPDs)[9,10] as they blend the electrical properties of metals with the benefits of polymers.[11] Among these, polymers with tricyclic fused aromatic compounds such as carbazole and fluorene, in the main chain have been well reported to possess excellent properties as materials for OLEDs.[12] Conventionally, it has been found that CPs are highly emissive in the dilute solutions but become nonemissive or weakly fluorescent in the thin solid films, which is a severe problem hindering the development of efficient PLEDs.[13]

Since the discovery of aggregation-induced emission (AIE) in 2001 by Tang et al., increasing attention has been paid in the synthesis of AIE molecules.[14] AIE is a phenomenon in which a luminogen, nonemissive in good solvents becomes highly emissive when aggregated in poor solvents or in thin films.[15] If a CP shows aggregation induced emission (AIE) property then the notorious fluorescence quenching in film form can be overcome.[16] The physical phenomenon for AIE is found to be the restriction of intramolecular rotation (RIR) in aggregated state, which leads to enhancement in fluorescence emission.[16] Since its discovery, increasing attention has been paid in the synthesis and development of AIE active conjugated polymers as they are rare, and can find intense application as PLED materials.[17]

Many groups have incorporated EDOT and fluorene in the backbone of numerous CPs. EDOT exhibits very high molar absorption coefficient (ε) and efficiently donates electrons owing to the presence of heteroatoms.[18–20(c)] Fluorene, conversely, apart from being a good hole transporter, has excellent chemical and thermal robustness and good solubility as well as high fluorescence quantum yield, high photoluminescence efficiency, and good photostability.[21–24] Polyfluorene is in general used as a blue emitter and by fusing it with other systems such as carbazole, the conjugation can be extended.[25] The carbazole moiety, apart from extending the conjugation, imparts excellent hole transporting property, high triplet energy, amorphous nature, and can be easily functionalized by reaction at the nitrogen atom. Moreover, on incorporation of carbazole, thermal and photochemical stability, and durability

Additional Supporting Information may be found in the online version of this article.

of the polymers were found to be significantly improved.[19,26,27] The presence of bulky cyano group in the CPs hinders π-π stacking and maintains coplanarity, which are essential factors for the formation of J-type aggregation leading to aggregation enhanced emission (AEE).[28,29]

The fusion of carbazole-fluorene or EDOT-fluorene in one molecule towards the enhancement of AEE in the solid state is well known.[23,30] However, the simultaneous incorporation of carbazole, fluorene, and EDOT in the same main chain along with a pendant cyano (CN) group toward developing an AEE chromophore has not been reported so far. This strategy can be very promising as the resulting polymers can exhibit tremendous potential toward development of PLED materials.

In this work, we report the synthesis and characterization of six polymers that have been designed to contain carbazole, fluorene, and EDOT repeat units in the main chain as well as a pendant cyano group with the specific aim of introducing AEE. To the best of our knowledge, this series of compounds has not been reported till date and the synthetic design, in principle, should enable potential toward PLED applications. The polymers were characterized in detail using spectroscopic tools and their properties were studied by UV–Visible/fluorescence spectroscopy and cyclic voltammetry. Theoretical studies were carried out using gas phase density functional theory (DFT) to get insight into the molecular arrangements and their energy levels.

EXPERIMENTAL

Chemicals

Palladium (II) chloride which was used to synthesize the catalyst $PdCl_2(PPh_3)_2$ and CuI were purchased from Sigma Aldrich and Finar & Co., respectively. The compound 3,4-ethylene dioxythiophene (**15,** CAS No. 126213-50-1) was purchased from Sigma Aldrich while 4,4'-dibromobiphenyl (**7**, CAS No. 92-86-4) and fluorene (**1**, CAS No. 86-73-7) were purchased from Alfa Aesar. All these chemicals were used as such without further purification. The solvents: DIPA, THF, DCM, and toluene were purchased from Rankem & Co. were distilled, where necessary, using standard procedures. The deuterated solvents were purchased from Merck & Co.

Synthesis of Precursors and Polymers

The dialdehyde (**18**) (new) was prepared using standard Sonogashira coupling reaction. The procedure is as follows: In a two-necked round bottom flask, the bromo compound (**17**) (6.83 mmol, 1 eq.), Pd(II) (5 mol %), and CuI (5 mol %) were dissolved in a 1:1 mixture of solvents (DIPA:THF) (total 50 mL) and degassed for 15 min using argon. Then, a degassed solution of the alkyne (**5**) (15.04 mmol, 2.2 eq.) in THF was added through a syringe to the reaction mixture at room temperature (final solvent ratio = 1:1). Then, the temperature was raised to 70 °C and maintained for 12 h. After the reaction, the solvents were evaporated under vacuum and the residue was extracted with DCM and water, washed with brine solution, dried with Na_2SO_4 and filtered. The solvent was removed under vacuum and the resulting crude product was purified by silica gel column chromatography (hexane/DCM 3/2) to give the dialdehyde (**18).** Yield: 88%, yellow solid. mp: 152 °C.

^{1}H NMR (400 MHz, $CDCl_3$, δ, ppm): 9.92 (s, 2H), 7.66 (d, $J = 8$ Hz, 2H), 7.53 (d, $J = 8$Hz, 2H), 7.45 (s, 2H), 4.40 (s, 8H), 1.94–1.98 (m, 4H), 1.03–1.22 (m, 20H), 0.80 (t, $J = 8$ Hz, 6H), 0.55 (s, 4H). ^{13}C NMR (125 MHz, $CDCl_3$, δ, ppm): 179.5, 151.3, 147.5, 143.5, 141.3, 131.0, 126.0, 121.0, 120.2, 118.1, 109.3, 101.7, 79.8, 65.1, 64.9, 55.4, 55.4, 40.3, 31.8, 31.8, 30.0, 29.3, 29.2, 23.7, 22.6, 22.5, 14.1, 14.1. IR (KBr, cm^{-1}): 2943, 2861, 2199, 1654, 1468, 1364, 1271, 1155, 1073, 957, 829, 678. UV–Vis (DCM) λ_{max}, nm: 392. MS (MALDI) *m/z*: 775.16 (100, M$^+$). Anal. Calcd for $C_{47}H_{50}O_6S_2$: C, 72.84; H, 6.50. Found: C, 73.17; H, 6.34.

Compound (**19**) (new) also a dialdehyde was synthesized by the same procedure as **18**. In this case, compound (**6**) was taken in place of (**5**). Yield: 77%, yellow solid. mp: 156 °C.

^{1}H NMR (400 MHz, $CDCl_3$, δ, ppm): 9.92 (s, 2H), 7.66 (d, $J=$ 8 Hz, 2H), 7.53 (dd, $J_1 = 8$ Hz, $J_2 = 1.2$ Hz, 2H), 7.50 (s, 2H), 4.33 (s, 8H), 1.94–1.98 (m, 4H), 1.03–1.24 (m, 28H), 0.80 (t, $J = 8$ Hz, 6H), 0.55 (s, 4H). ^{13}C NMR (125 MHz, $CDCl_3$, δ, ppm): 179.6, 151.4, 147.6, 143.6, 141.5, 131.1, 126.1, 121.1, 120.3, 118.2, 109.5, 101.8, 80.0, 65.3, 65.0, 55.6, 40.4, 32.0, 30.1, 30.1, 29.7, 29.6, 29.6, 29.4, 29.3, 23.9, 22.7, 14.2. IR (KBr, cm^{-1}): 2931, 2850, 2211, 1654, 1503, 1457, 1364, 1259, 1155, 1085, 969, 806, 678. UV–Vis (DCM) λ_{max}, nm: 392. MS (MALDI) *m/z*: 831.30 (100, M$^+$). Anal. Calcd for $C_{51}H_{58}O_6S_2$: C, 73.70; H, 7.03. Found: C, 73.81; H, 7.18.

The monomer (**M1)** (new) was synthesized using standard Knoevenagel condensation reaction. The procedure is as follows: In a round bottom flask containing the dialdehyde (**18**) (5.6 mmol, 1 eq.), THF (100 mL) was added followed by the addition of 4-bromophenyl acetonitrile (**20**) (12.3 mmol, 2.2 eq.) and aqueous solution of NaOH (22.5 mmol in 10 mL H_2O, 4 eq.). The resulting mixture was stirred at 70 °C for 18 h. After the reaction, the solvent was evaporated under vacuum and the residue was extracted with DCM and water, washed with brine solution, dried with Na_2SO_4 and filtered. After removing the solvent, the crude product was purified by silica gel column chromatography (hexane/DCM 3/7) to give monomer (**M1**). Yield: 83%, red solid. mp: 274 °C.

^{1}H NMR (400 MHz, $CDCl_3$, δ, ppm): 7.72 (s, 2H), 7.66 (d, $J = 8$ Hz, 2H), 7.47–7.54 (m, 12H), 4.36 (s, 8H), 1.96–1.99 (m, 4H), 1.05–1.22 (m, 20H), 0.81–0.86 (m, 6H), 0.58 (s, 4H). ^{13}C NMR (125 MHz, $CDCl_3$, δ, ppm): 151.2, 143.8, 143.1, 141.1, 133.1, 132.2, 132.1, 132.1, 130.7, 129.1, 126.9, 126.9, 126.8, 125.9, 122.7, 121.3, 120.1, 118.3, 114.4, 104.4, 104.0, 101.5, 80.3, 65.0, 65.0, 55.3, 40.3, 31.7, 30.0, 29.3, 29.2, 23.8, 22.6, 14.0. IR (KBr, cm^{-1}): 2943, 2850, 2211, 1584, 1457, 1387, 1317, 1073, 1003, 957, 829. UV–Vis (DCM) λ_{max}, nm: 444. MS (MALDI) *m/z*: 1130.15 (100, M$^+$). Anal. Calcd for $C_{63}H_{58}Br_2N_2O_4S_2$: C, 66.90; H, 5.17; N, 2.48. Found: C, 66.95; H, 4.50; N, 2.32

Monomer (**M2)** (new) was synthesized following the same procedure as (**M1**) only compound (**19)** was taken in place of (**18**). Yield: 34%, red solid. Mp: 230 °C.

^{1}H NMR (400 MHz, $CDCl_3$, δ, ppm): 7.73 (s, 2H), 7.67 (d, $J = 8$ Hz, 2H), 7.48–7.55 (m, 12H), 4.39–4.36 (m, 8H), 1.96–2.00 (m, 4H), 1.06–1.25 (m, 28H), 0.84 (t, $J = 6.8$ Hz, 6H), 0.59 (s, 4H). ^{13}C NMR (125 MHz, $CDCl_3$, δ, ppm): 151.2, 143.8, 143.1, 141.1, 133.1, 133.0, 132.2, 132.1, 132.1, 130.7, 129.1, 126.9, 126.9, 126.8, 125.9, 122.7, 121.3, 120.1, 118.3, 114.4, 104.4, 104.0, 101.5, 80.3, 65.0, 65.0, 55.3, 40.3, 31.7, 30.0, 29.7, 29.6, 29.6, 29.5, 29.4, 29.3, 29.2, 23.8, 22.6, 14.0. IR (KBr, cm^{-1}): 2924, 2852, 2204, 1556, 1500, 1447, 1407, 1403, 1361, 1307, 1255, 1087, 1005, 950, 820. UV–Vis (DCM) λ_{max}, nm: 445. MS (MALDI) *m/z*: 1186.24 (100, M$^+$). Anal. Calcd for $C_{67}H_{66}Br_2N_2O_4S_2$: C, 67.78; H, 5.60; N, 2.36. Found: C, 67.89; H, 4.71; N, 2.22.

General Procedure for the Synthesis of Polymers P1–P6

The polymers (**P1–P6**) were prepared using standard Sonogashira coupling reaction. The general procedure is as follows: In a two-necked round bottom flask, the monomers (**M1** or **M2** as the case may be) (0.67 mmol, 1 eq.), Pd(II) (5 mol %), and CuI (5 mol %) were dissolved in a 1:1 mixture of solvents (DIPA:Toulene) (total 60 mL) and degassed for 15 min using argon. Then, a degassed solution of the dibromocarbazoles (**12** or **13** or **14**) (0.67 mmol, 1 eq.) in THF was added to the reaction mixture at room temperature (final solvent ratio = 1:1). Then, the temperature was raised to 70 °C and maintained for 24 h. After the reaction, the solvents were evaporated under vacuum and the residue was extracted with DCM and water, washed with brine solution, dried with Na_2SO_4 and filtered. The solvent was removed under vacuum and the resulting crude product was purified by soxhlet extraction using hexane, methanol and chloroform to give the polymers (**P1–P6**).

P1: Yield: 69%, red solid. ^{1}H NMR (400 MHz, $CDCl_3$, δ, ppm): 7.65–7.66 (d), 7.52–7.60 (m), 7.34–7.46 (m), 7.25–7.28 (m), 4.23–4.32 (m), 1.82–1.92 (m), 1.56 (s), 1.34–1.38 (m), 0.89–1.26 (m), 0.72–0.76 (m). IR (KBr, cm^{-1}): 2931, 2861, 2222, 1596, 1491, 1364, 1259, 1085, 1015, 945, 818. UV–Vis (DCM) λ_{max}, nm: 447. Monomer ratio in the polymer by ^{1}H NMR: 1.5:1.0 (**M1:12**).
P2: Yield: 49%, red solid. ^{1}H NMR (400 MHz, $CDCl_3$, δ, ppm): 7.66 (s), 7.54–7.60 (m), 7.41–7.47 (m), 7.36 (s), 7.26–7.27 (d), 4.26–4.32 (m), 1.85–1.92 (m), 1.57 (s), 0.95–1.20 (m), 0.71–0.75 (m), 0.46–0.51 (m). IR (KBr, cm^{-1}): 2943, 2850, 2199, 1596, 1468, 1375, 1096, 1003, 945, 818. UV–Vis (DCM) λ_{max}, nm: 447. Monomer ratio in the polymer by ^{1}H NMR: 1.5:1.0 (**M1:13**).
P3: Yield: 62%, red solid. ^{1}H NMR (400 MHz, $CDCl_3$, δ, ppm): 7.65–7.66 (d), 7.55–7.61 (m), 7.36–7.48 (m), 7.26–7.28 (m), 4.27–4.33 (m), 1.86–1.92 (m), 1.50 (s), 0.96–1.20 (m) 0.73–0.76 (m), 0.46–0.51 (m). IR (KBr, cm^{-1}): 2931, 2850, 2211, 1608, 1457, 1375, 1271, 1096, 1027, 969, 829 cm^{-1}. UV–Vis (DCM) λ_{max}, nm: 445. Monomer ratio in the polymer by ^{1}H NMR: 2.0:1.0 (**M1:14**).
P4: Yield: 45%, red solid. ^{1}H NMR (400 MHz, $CDCl_3$, δ, ppm): 8.02–8.05 (m), 7.24–7.79 (m), 4.34–4.40 (m), 1.91–1.99 (m), 1.59 (s), 1.00–1.34 (m), 0.81–0.91 (m), 0.53–0.58 (m). IR (KBr, cm^{-1}): 2915, 2839, 2217, 1580, 1489, 1352, 1292, 1246, 1079, 973, 806. UV–Vis (DCM) λ_{max}, nm: 453. Monomer ratio in the polymer by ^{1}H NMR: 1.0:1.0 (**M2:12**).
P5: Yield: 49%, a red solid. ^{1}H NMR (400 MHz, $CDCl_3$, δ, ppm): 7.73 (s), 7.67 (d), 7.48–7.55 (m), 4.36–4.39 (m), 4.33 (s), 1.96–2.00 (m), 1.06–1.25 (m), 0.84 (t), 0.59 (s). IR (KBr, cm^{-1}): 2943, 2850, 2211, 1584, 1468, 1352, 1259, 1096, 1003, 945, 829. UV–Vis (DCM) λ_{max}, nm: 451. Monomer ratio in the polymer by ^{1}H NMR: 2.0:1.0 (**M2:13**).
P6: Yield: 56%, a red solid. ^{1}H NMR (400 MHz, $CDCl_3$, δ, ppm): 8.02–8.05 (m), 7.34–7.79 (m), 4.34–4.39 (m), 1.88–1.99 (m), 1.59 (s), 1.62 (s), 1.00–1.26 (m), 0.80–0.88 (m), 0.52–0.58 (m). IR (KBr, cm^{-1}): 2931, 2850, 2199, 1596, 1561, 1468, 1375, 1329, 1271, 1085, 1015, 945. UV–Vis (DCM) λ_{max}, nm: 425. Monomer ratio in the polymer by ^{1}H NMR: 1.8:1.0 (**M2:14**).

RESULTS AND DISCUSSION

Synthesis and Characterization

Toward the synthesis of the CPs, dialdehydes **18, 19** were synthesized as shown in Scheme 1. The dialdehydes in turn were synthesized from the dialkynedialkylfluorenes **5**, **6** that in turn were obtained via Sonogashira reaction from 2,7-dibromodialkylfluorene **3**. The dibromodialkylfluorene **3** was synthesized by the alkylation of dibromofluorene **2**, which in turn was synthesized from fluorene **1**. The alkyl groups were attached to increase the solubility of the polymers in common organic solvents. The bromoaldehyde **17** was obtained by the bromination of **16,** which in turn, was obtained by the formylation of EDOT **15**. Then, bromoaldehyde **17** was reacted with dialkynedialkylfluorenes **5**, **6** to give the dialdehydes **18** and **19** via Sonogashira coupling reactions, which were further converted to the dibromomonomers **M1**, **M2** via Knoevenagel condensation reaction between 4-bromophenylacetonitrile **20** and the dialdehydes **18**, **19**. The dialdehydes were obtained in 88% **18** and 77% **19** yields, whereas the yields for monomers **M1** and **M2** were 83% and 34%, respectively. All these compounds were thoroughly characterized by ^{1}H NMR, ^{13}C NMR, MALDI, and CHN analysis as detailed in the Supporting Information. The structures of the starting compounds and the dialdehydes **18**, **19** were characterized by spectroscopic tools and found to be consistent with that expected for the given structures (please see characterization data shown in Supporting Information Figs. S1–S12 along with the peak assignments). Monomers **M1** and **M2** were also synthesized as shown in Scheme 1. The structure of the monomers **M1**, **M2** were characterized by spectroscopic tools and they were found to be consistent with that expected for the given structures (please see characterization data shown in Supporting Information Figs. S13–S24). The compounds **12, 13, 14** were synthesized from 4, 4'-dibromobiphenyl **7** through standard protocols as shown in Scheme 1.

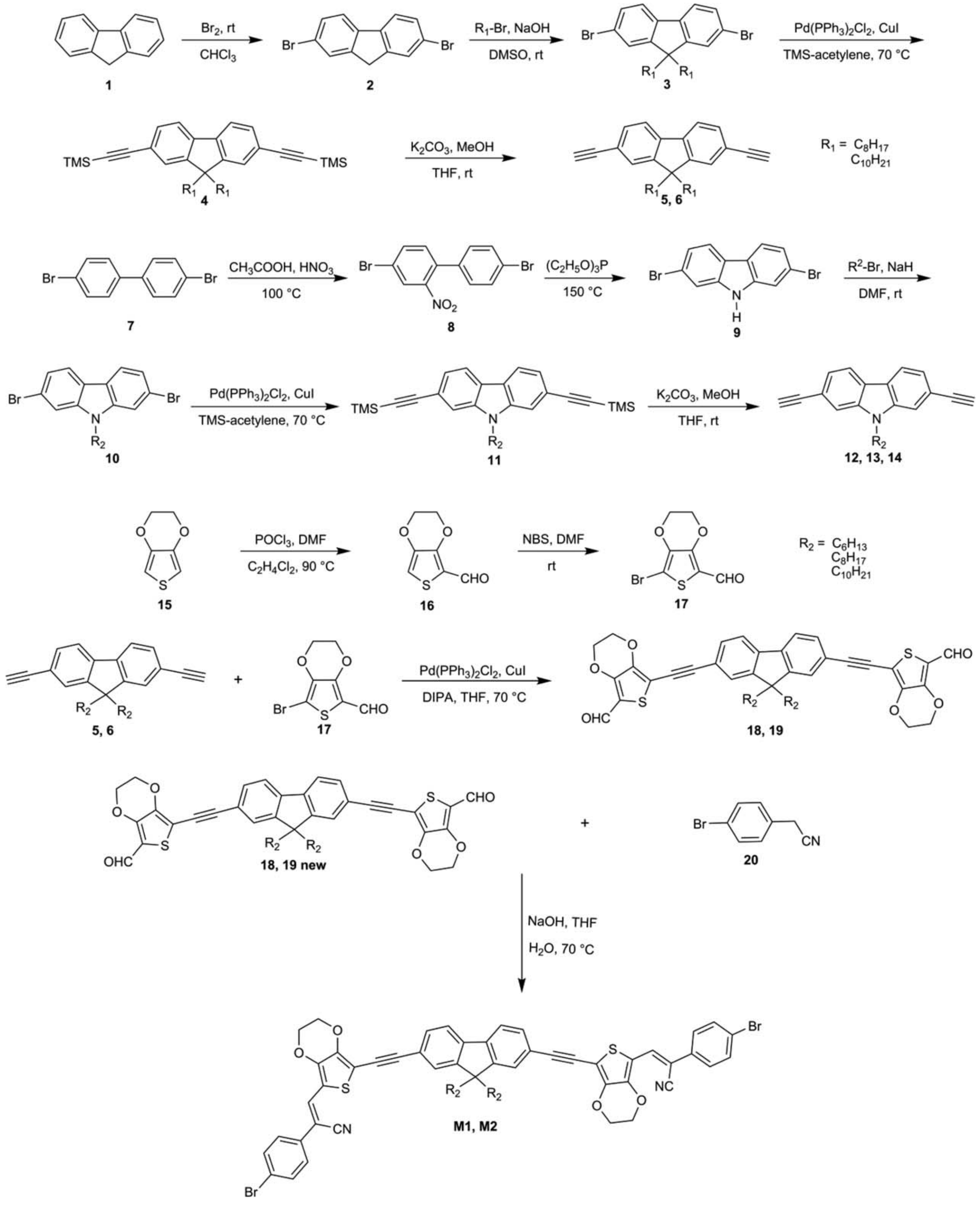

SCHEME 1 Synthetic route for monomers **M1** and **M2.**

Polymers **P1–P6** were synthesized by the Sonogashira coupling as shown in Scheme 2. The low yield of the polymers (47–62%) in all the cases suggested that the coupling reaction was not efficient from the polymerization point of view. The yield of the polymers could be improved by driving out the solvent as the polymerization proceeded. Thus, a yield of 69% for polymer **P1** has been obtained under these conditions, when the polymerization was carried out for 5 days. The ^{1}H NMR and ^{13}C NMR of the polymers are shown in Supporting Information Figures S25–S30. The peak

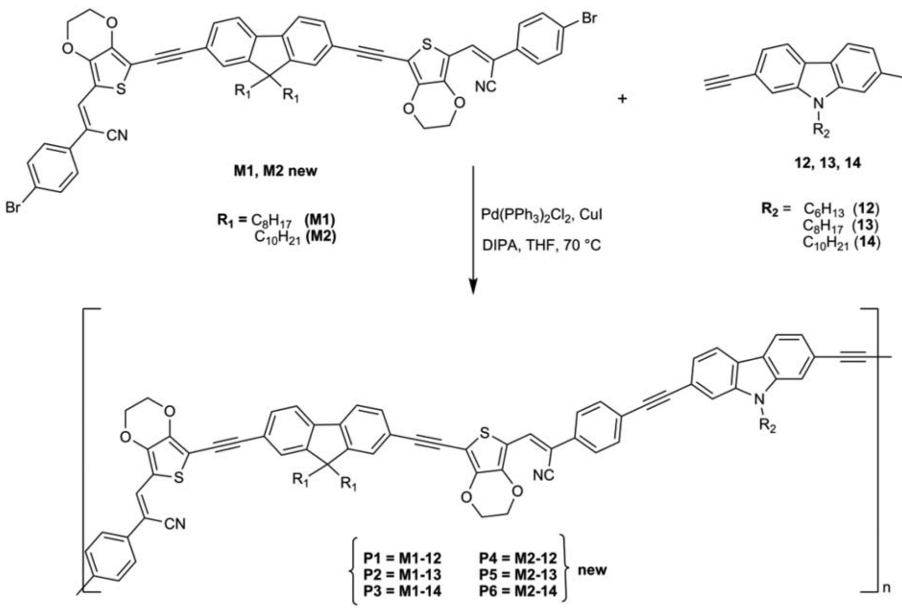

SCHEME 2 Synthetic route for polymers **P1–P6.**

assignments are also shown in the corresponding figures. The disappearance of the acetylenic proton (peak at 3.2 ppm in ^{1}H NMR) of the monomers suggests the formation of polymers.

The number average molecular weight (M_n) and polydispersity index (PDI) values of the polymers as ascertained by gel permeation chromatography (GPC) using narrow molecular weight polystyrene standards are given in Table 1. The ratio of the monomer composition in the polymers, as ascertained by ^{1}H NMR is also given in Table 1. The method used to calculate the monomer ratios is discussed in Supporting Information Fig. S31. For the purpose of clarity, ^{1}H NMR of polymer **P6** along with specific peak assignments is also included in Supporting Information Fig. S31.

Photophysical Studies

The absorption spectra of the monomers (**M1** and **M2** in DCM) showed absorption maxima at 444 nm and 445 nm, respectively, which could be attributed to π-π^* transition (Supporting Information Fig. S32). A red shift of around 100 nm was observed in the λ_{max} of the monomers, which resulted due to the extension of the conjugation through the attachment of EDOT and carbazole moieties to fluorene (λ_{ma} value for pure fluorene was observed at 320 nm, while that for EDOT is 260 nm).[31] When compared to the premonomers **18** and **19**, the monomers showed a red shift of 53 nm. This implies that the extent of conjugation is increased by attaching 4-bromophenylacetonitrile, as expected. In polystyrene film, the monomers **M1** and **M2** showed absorption maxima at 445 nm and 439 nm, respectively (Supporting Information Fig. S32); they were not significantly different from what was observed in solution. The emission maxima of the monomers in DCM solution (for excitation wavelength of 444 nm and 445 nm, respectively) were 510 nm and 511 nm for **M1** and **M2**, respectively. Apart from the prominent peaks, shoulder peaks were observed at 539 nm and 581 nm. In polystyrene matrix, the emission maxima of the monomers were 504 nm and 513 nm, respectively (Supporting Information Fig. S32). Apart from this, prominent shoulder peaks at 524 nm, 574 nm for **M1** and 520 nm and 580 nm for **M2** were also observed. However, in the pristine powder form, the emission maxima of the monomers were 627 nm and 604 nm for **M1** and **M2**, respectively, (Supporting Information Fig. S33). This may be attributed to their aggregation which restricts the rotation of the polymer backbone and improves the effective conjugation leading to the red shifted absorption and emission maxima. The absorption and emission spectra of all the polymers in DCM solution are shown in Figures 1 (**P1–P3**) and 2 (**P4–P6**). The polymers, **P1–P6**, exhibited broad absorption band with maxima between 447 nm to 453 nm. The absorption maxima of the polymers remained the same as the monomers, although broadening of peaks

TABLE 1 Number Average Molecular Weight (M_n), Polydispersity Index (PDI) of the Polymers and Molar Ratios of the Comonomers in the Polymers

Cmp	M_n (Daltons)	PDI	Composition (^{1}H NMR)
P1	6000	NA	1.5(**M1**):1.0(**12**)
P2	5900	1.39	1.5(**M1**):1.0(**13**)
P3	9800	1.65	2.0(**M1**):1.0(**14**)
P4	5700	2.34	1.0(**M2**):1.0(**12**)
P5	6800	3.25	2.0(**M2**):1.0(**13**)
P6	6000	1.75	1.8(**M2**):1.0(**14**)

Note: For **P2** and **P3** the concentration of the higher molecular weight polymer fragment was lower than the concentrations of the oligomers as inferred from GPC chromatograms.

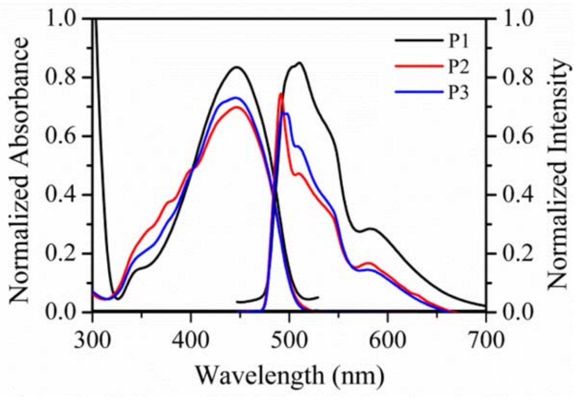

FIGURE 1 UV–Visible absorption and emission ($\lambda_{exc}=\lambda_{max}$) spectra of **P1–P3** in DCM. [Color figure can be viewed in the online issue, which is available at wileyonlinelibrary.com.]

was observed. Moreover, **P1–P6** showed multiple absorptions (five peaks) below λ_{max} in DCM. This was more prominent in **P4–P6.** These broadening can be due to the absorption from different segments of the polymers, which is a general phenomenon in case of CPs. The optical band gap (E_g) of the polymers (**P1–P6)** was determined from the onset of absorbance using the formula $E_{gap} = 1242/\lambda_{onset}$ (**1**) and found to be ranging between 2.35 and 2.42 eV, which was essentially independent of the nature of the side chain. The polymers **P4–P6** showed lower energy band gap (0.08 eV) than those of **P1–P3**. This indicates that the variation of R-group may have detrimental effect on the band gap energy.

In polystyrene film, the polymers **P1–P3** showed absorption maxima at 420 nm, 419 nm, 439 nm, while polymers **P4–P6** showed absorption maxima at 447 nm, 419 nm, 421 nm, respectively (Supporting Information Fig. S32). Thus, there is not much change as we compare the absorption maxima of molecules in DCM solution to those in the polystyrene matrix although the λ_{max} decreases slightly in polymer matrix.

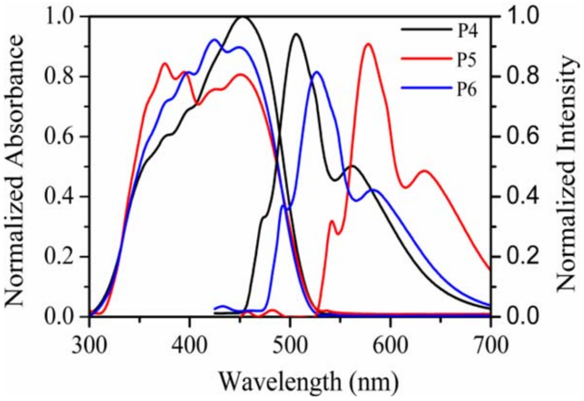

FIGURE 2 UV–Visible absorption and emission ($\lambda_{exc}=\lambda_{max}$) spectra of **P4–P6** in DCM. [Color figure can be viewed in the online issue, which is available at wileyonlinelibrary.com.]

The emission maxima for the polymers **P1, P2,** and **P3** were observed between 492 and 510 nm, while those for the polymers **P4, P5,** and **P6** were observed between 506 and 578 nm, respectively, in DCM solution (Figs. 1 and 2). These values correspond to green emission as can be seen in the photographs [Fig. 3(a)]. The polymers also exhibited significant shoulder peaks similar to those of the monomers, which might be attributed to the aggregation. Since minimal overlap is observed between the absorption and emission spectra of both the monomers and polymers, insignificant Forster energy transfer is expected under some perturbation (pH change, doping, etc.), which is desirable for PLED applications.[32] The fluorescence quantum yields in the solution state (Fluorescein standard) for polymers **P2** and **P5** were found to be 41% and 43%, respectively.[33]

In PS matrix, the emission maxima for polymers **P1, P2,** and **P3** in PS matrix were centred on 529 nm with a prominent shoulder peak around 580 nm (Supporting Information Fig. S32). Those for **P4, P5,** and **P6** were observed between 502 and 533 nm with prominent shoulder peak at around 580 nm (Supporting Information Fig. S32). Photographs of the emission in the thin film form are shown in Figure 3(b) for **P1–P6** in PS matrix. The emission maximum is significantly enhanced and red shifted from 5 to 37 nm in film state, owing to the efficient π-π stacking and increase in effective conjugation in the film state due to freezing of the segmental motion in PS matrix (with a T_g of 95 to 100°C). This is another evidence for the chromophores exhibiting excellent AEE.

The photographs of **P1–P6** under UV light irradiation in the solid state are shown in Figure 3(c). The emission maxima in powder form for **P1, P2, P3** polymers were 599 nm, 617 nm, and 623 nm (Supporting Information Fig. S33), while those for **P4, P5,** and **P6**, were 603 nm, 594 nm, and 594 nm (Supporting Information Fig. S33), respectively. In addition to the main emission peak, the three polymers exhibited shoulder peaks. There was remarkable red shift of 117 nm, 93 nm, 89 nm, 125 nm, 129 nm, 97 nm, 16 nm, and 68 nm for **M1, M2, P1, P2, P3, P4, P5, and P6,**

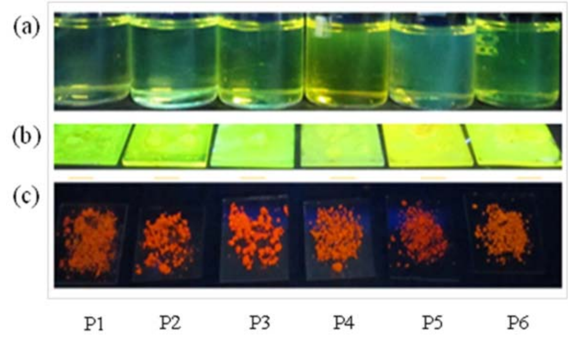

FIGURE 3 Photos of **P1–P6** taken in (**a**) solution state (**b**) PS matrix and (**c**) solid state under UV lamp. [Color figure can be viewed in the online issue, which is available at wileyonlinelibrary.com.]

TABLE 2 Absorption and Emission Spectral Data for M1, M2, and P1–P6

	$\lambda_{max}{}^{a}$ (abs.)		$\lambda_{max}{}^{b}$ (em.)		
Cmp	DCM	PS Matrix	DCM	PS Matrix	Solid
M1	444	445	510	504	627
M2	445	439	511	513	604
P1	447	420	510	529	599
P2	447	419	492	529	617
P3	445	439	494	529	623
P4	453	447	506	502	603
P5	451	419	578	533	594
P6	425	421	526	531	594

[a] Absorption maximum at the longest wavelength.
[b] Emission maximum on photoexcitation.

respectively, in the λ_{max} in the solid state compared to their solution maxima. The bathochromic shift in the powder form was even more remarkable. This substantial red shift observed in the powder form when compared to solution and polystyrene matrix shows that in polystyrene matrix the stacking and intermolecular interaction are not as pronounced as in the powder form, where the molecules are at close proximity to each other. The photophysical data is summarized in Table 2.

AEE Studies

To explore the AEE properties of these polymers, we carried out the aggregation studies of the polymers. The photoluminescence (PL) spectra of polymer **P1** in THF/water mixtures with 0 to 90% water fractions is shown in Figure 4. It can be seen that the emission remains the same till 50% water fraction, as in THF, which means the solute resists the formation of aggregate. But when the water fraction was increased beyond 50%, (from 60% to 90%), the intensity of fluorescence increased significantly along with considerable red shift and reached the maximum intensity when the water fraction was 90%. This indicates that the polymer **P1** shows aggregation enhanced emission (AEE) on addition of a non-solvent, such as water, which increases the polarity of the solution. The emission intensity increased 2.6 fold (Fig. 5) when water fraction was 90% as compared to that in pure THF solution. The emission color shifted from green to orange. The red shifted emission may be attributed to the enhanced planarization of the polymer backbone, which increases the effective π-conjugation.

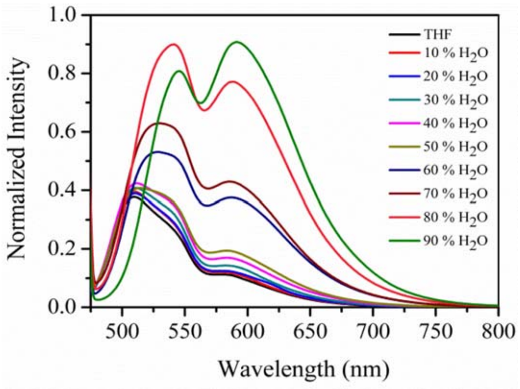

FIGURE 4 Changes in the emission spectrum of **P1** in THF/water mixture with different water volume fractions 0–90%. [Color figure can be viewed in the online issue, which is available at wileyonlinelibrary.com.]

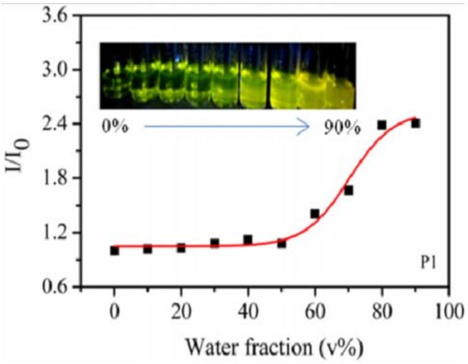

FIGURE 5 Variation in the integrated PL intensity of **P1** with increasing water fractions in THF. Inset depicts snapshots of **P1** taken under UV light in the THF–water mixture with different water volume fractions 0–90%. Left to right, increase in water fraction. [Color figure can be viewed in the online issue, which is available at wileyonlinelibrary.com.]

The aggregation enhanced emission (AEE) may be caused due to restriction of intramolecular rotation (RIR).[34,35] Thus, the RIR is effectively restricting the nonradiative decay channels leading to enhanced emission in THF/water mixture. From the emission spectra and the AEE studies, it can be concluded that the polymer **P1** shows enhanced fluorescence in aggregated state and its emission lies in the green to yellow region of the electromagnetic spectrum. The enhancement in fluorescence with increase in water fraction is shown in inset of Figure 5.

The aggregation of the polymer particles in water-THF mixture was further confirmed by DLS (dynamic light scattering) (Supporting Information Fig. S35) and SEM (scanning electron microscopy) (Fig. 6) analyses. The average radius of the aggregates decreased progressively from 751 nm, 292 nm, 292 nm, 327 nm, 226 nm to 157 nm as the vol % of water

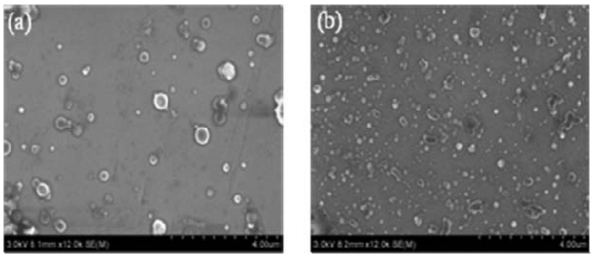

FIGURE 6 SEM images of **P1** in THF–water mixture (**a**) 50:50 v/v and (**b**) 20:80 v/v.

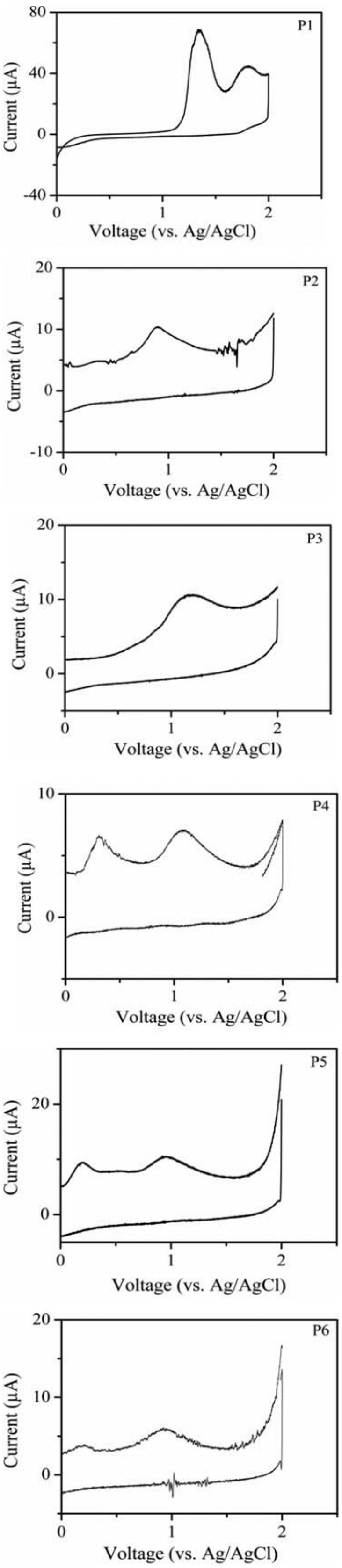

FIGURE 7 Cyclic voltammograms of **P1–P6** in film form (cathodic region) by drop casting polymers from DCM solution on working electrode (0.1 M Bu_4NPF_6 as supporting electrolyte.

was increased from 40%, 50%, 60%, 70%, 80% to 90%, respectively. The size of the aggregates decreases with increasing water fraction because of the rapid reduction in the solvating power of the solvent mixture that is supported by SEM images [Figs. 6(a) for 50% water and 6(b) for 80% water]. This observation has been well reported.[29,36(a,b)]

The AEE studies for other polymers **P2–P6** were also carried out and found to show similar patterns. The increase in emission intensities are 2.3, 2.7, 1.7, 1.5, and 1.3 folds for polymers **P2**, **P3**, **P4**, **P5,** and **P6**, respectively, when water fraction is 90% as compared to that in pure THF solution. The details can be found in Supporting Information Figure S34.

Electrochemical Properties

The electrochemical behavior of the monomers and polymers was investigated both in DCM solution (Supporting Information Fig. S36) and in film form (Fig. 7 for polymers and Supporting Information Fig. S37 for monomers) from the cyclic voltammograms (CV). The films were formed by drop casting monomer and polymer films from DCM solution on the working electrode containing 0.1 M n-Bu_4NPF_6 as a supporting electrolyte. The HOMO-LUMO energy gaps and the energy levels of the compounds were determined by using optical and electrochemical methods, which are summarized in Table 3 for film form and in Supporting Information Table S1 in DCM solution. The CV of monomers and polymers envisaged an irreversible oxidation process with E_{onset} oxidation in the range 0.55–1.11 V in the film form and 0.86–1.38 V in DCM solution. The onset of oxidation peak can be attributed to the formation of mono radical cation of the monomers and the polymers. The lower oxidation potential can be due the presence of carbazole, which is known to form radical cation easily (because of the presence of nitrogen atom). These low oxidation values also support that these polymers may serve as good hole transporting materials in

TABLE 3 The Optical Band Gap and Electrochemical Data of Monomers M1, M2, and Polymers P1–P6

Cmp	E_{gap}[a]	HOMO[b]	LUMO[c]	E_{gap}[d]
M1	2.44	−5.56	−3.08	2.51
M2	2.44	−5.50	−3.14	2.36
P1	2.42	−5.43	−3.16	2.27
P2	2.43	−5.01	−3.08	1.93
P3	2.43	−4.94	−3.06	1.88
P4	2.35	−5.19	−3.14	2.05
P5	2.35	−5.15	−3.09	2.06
P6	2.35	−4.99	−3.09	2.05

[a] Energy band gap calculated from λ_{onset} in eV;.

[b] HOMO energy level calculated using the equation $E_{\text{HOMO}} = -(E^{\text{OX}} + 4.39)$ eV (**2**);.

[c] LUMO energy level calculated using the equation $E_{\text{LUMO}} = -(E^{\text{red}} + 4.39)$ eV (**3**);.

[d] Energy band gap calculated from CV in eV by drop casting films of monomers and polymers films from DCM solution on the working electrode, the HOMO and LUMO were also calculated for the same.

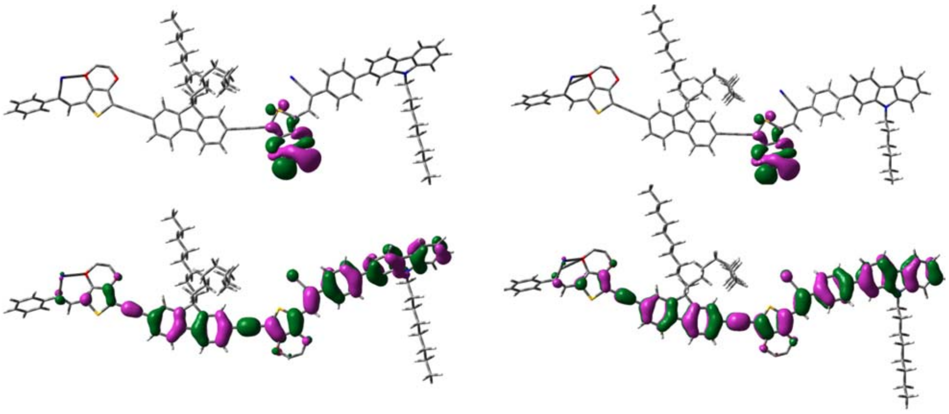

FIGURE 8 B3LYP/6-31G* DFT calculated HOMO (bottom) and LUMO (top) contours of **P2** (left) and **P5** (right). [Color figure can be viewed in the online issue, which is available at wileyonlinelibrary.com.]

photovoltaics. The onset potentials for polymers were 0.41 eV less than those of monomers in the film form, which signify the importance of incorporating carbazole in the polymeric backbone. The irreversible reduction process with E_{onset} reduction in the range 1.23–1.33 V in film form and 1.11–1.34 V in DCM solution can be due to the formation of radical anions. The higher values for reduction onsets as compared to oxidation onsets reveal that it is easier to oxidize these molecules and hence they can function better as hole transporters than electron transporters. The redox potential of Fc/Fc$^+$ (standard value = 4.8 eV with respect to vacuum) was observed at 0.41 V in 0.10 M tetrabutyl ammonium hexaflurophosphate/DCM solution. Based on this the HOMO and LUMO energy levels of the monomers and polymers were estimated using the following equation:[37]

$$E_{\mathrm{HOMO}} = -\left(E^{\mathrm{OX}} + 4.39\right)\ \mathrm{eV} \tag{2}$$

$$E_{\mathrm{LUMO}} = -\left(E^{\mathrm{red}} + 4.39\right)\ \mathrm{eV} \tag{3}$$

where E^{OX} and E^{red} are the onset potentials of oxidation and reduction, respectively, as measured against Ag/AgCl reference. The HOMO energy levels of the monomers and polymers were found to be in the range −4.94 eV to 5.56 eV in film form and −5.25 to −5.77 eV in DCM solution and the LUMO energy levels ranged from −3.06 eV to −3.16 eV in film form and −3.05 to 3.28 eV in DCM solution. Thus, the energy band gaps calculated in film form are less than those in DCM solution. Moreover, in film form the difference in the band gaps of monomers was 0.39 eV more than the band gaps in the polymers. This indicates the increase in conjugation on polymerization. The electrochemical band gaps of the monomers and polymers, calculated from the onset potentials of the oxidation and reduction, were lower than the values obtained from the optical band gap. This difference can be due to the interface between the electrodes and the molecules in the electrochemical system, which is absent in the optical system. Since the PLED configuration is very similar to the electrochemical system, the data calculated from electrochemical method are more acceptable from the device design point of view. Moreover, the HOMO energy levels of the polymers were approximately 0.41 eV in film form and 0.25 eV in DCM solution, lower than those of monomers. Similarly, LUMO energy levels of the polymers were also found to be lower than those of monomers. Thus, polymerization has effectively increased the conjugation which is altering the energy levels.

Computational Studies

Gas phase density functional theory (DFT) calculations (B3LYP/6-31G* level) were carried out to get insight into the electronic distribution in the polymers. The DFT generated HOMO and LUMO levels were also calculated and compared with the experimentally determined values. The HOMO, LUMO patterns of polymers **P1** and **P5** are shown in Figure 8.

In all the polymers, the HOMO is mainly located on the fluorene and carbazole rings and the LUMO is primarily located on the oxygen atoms of EDOT. In both **P2** and **P5** the HOMO energy level is 5.52 eV while LUMO energy level is 3.31 eV and the energy band gap is 2.1 eV. These values are comparable (with slight difference) to the experimentally determined values.

Thermal Properties

The thermal properties of the target compounds were determined by thermogravimetric analysis (TGA) (Supporting Information Figs. S38, S39; Tables S2 and S3). The monomers as well as all the polymers showed very high thermal stability with a decomposition temperature of 390 and 397 °C, respectively, at 5% weight loss for monomers **M1** and **M2** while the decomposition temperatures observed for polymers **P1, P2, P3, P4, P5,** and **P6** were 365, 391, 402, 389, 410, and 405 °C, at 5% weight loss, respectively. The thermal decomposition peak for pure PF is 448 °C. The high thermal stability observed is due to the fused aromatic system. Such high thermal robustness is essential when PLEDs are fabricated, and for the device lifespan.

PXRD of Monomers and Polymers

The powder XRD (PXRD) pattern of the monomers **M1** and **M2** (Supporting Information Fig. S40) and the polymers **P1** to **P6** (Supporting Information Fig. S41) showed that the polymers were highly amorphous in the solid state suggesting that dissolution as well as film forming tendency (especially in combination with high molecular weight) could be expected. These amorphous polymers can be advantageously used in the fabrication of light emitting diodes as crystalline materials are not so preferred for the same. In contrast, the PXRD pattern of the monomers (**M1** and **M2**) showed that both the monomers are crystalline in nature as can be seen by the sharp peaks with narrow peak width.

CONCLUSIONS

We have synthesized six new conjugated polymers with carbazole, fluorene, EDOT, acetylene, phenylene, and ethylene moieties along the main chain and a cyano pendant group attached to the ethylene moiety. Palladium catalysed Sonogashira coupling reaction was used as the tool and the polymers were characterized thoroughly using various spectroscopic analyses. The polymers **P1–P6** in solution and in PS matrix show emission in green region while it is red in the solid state. Aggregation enhanced emission (AEE) properties were also observed as expected from the synthetic design considerations. Furthermore, the AEE studies showed that a 2.6 fold increase in fluorescence intensity was observed in 90:10 THF/water mixture as compared to pristine THF solution of polymer **P1**. The AEE property was further verified by DLS and SEM studies. The band gaps of the polymers were assessed by optical, electrochemical, and computational studies (gas phase density functional theory [DFT]). Optical and electrochemical characterizations have shown that the energy band gaps (2.35–2.44 eV) and energy levels of the polymers are suitable for their application as thin film PLED materials. Additionally, the presence of carbazole and EDOT in the polymer backbone makes these polymers better hole transporting materials. The LED fabrication and studies for the same are under progress and will be reported in near future.

ACKNOWLEDGMENTS

This work was supported by Indian Institute of Technology, Madras (IITM), India. We thank the Department of Chemistry and especially Prof. Prasad for the support in doing DLS studies. Timely help from Sitakant Satpathy in DFT studies is heartily acknowledged.

REFERENCES AND NOTES

1 (a) M. Sassi, M. M. Salamone, R. Ruffo, C. M. Mari, G. A. Pagani, L. Beveria, *Adv. Mater.* **2012**, *24*, 2004–2008; (b) R. H. Friend, R. W. Gymer, A. B. Holmes, J. H. Burroughes, R. N. Marks, C. Taliani, D. D. C. Bradley, D. A. Dos Santos, J. L. Bredas, M. Logdlund, W. R. Salaneck, *Nature* **1999**, *397*, 121–128.

2 A. Kraft, A. C. Grimsdale, A. B. Holmes, *Angew. Chem. Int. Ed.* **1998**, *37*, 402–428.

3 X. Y. Deng, *Int. J. Mol. Sci.* **2011**, *12*, 1575–1594.

4 S. J. Ananthakrishnan, E. Varathan, E. Ravindran, N. Somnathan, V. Subramanian, A. B. Mandal, J. D. Sudha, R. Ramakrishnan, *Chem. Commun.* **2013**, *49*, 10742–10744.

5 C. D. Dimitrakopoulos, P. R. L. Malenfant, *Adv. Mater.* **2002**, *14*, 99–117.

6 W. Wu, Y. Liu, D. Zhu, *Chem. Soc. Rev.* **2010**, *39*, 1489–1502.

7 G. Horowitz, *Adv. Mater.* **1998**, *10*, 365–377.

8 (a) L. L. Zhou, M. Li, H. Y. Lu, C. F. Chen, *Polym. Chem.* **2016**, *7*, 310–318; (b) H. N. Kim, Z. Guo, W. Guo, W. Zhu, J. Yoon, H. Tian, *Chem. Soc. Rev.* **2011**, *40*, 79–93.

9 C. J. Brabec, N. S. Sariciftci, J. C. Hummelen, *Adv. Funct. Mater.* **2001**, *11*, 15–26.

10 C. Winder, N. S. Saricftci, *J. Mater. Chem.* **2004**, *14*, 1077–1086.

11 A. K. Bakshi, G. Bhalla, *J. Sci. Ind. Res.* **2004**, *63*, 715–728.

12 K. H. Lee, K. Morino, A. Sudo, T. Endo, *Polym. Bull.* **2011**, *67*, 227–236.

13 L. B. Xing, X. J. Wang, J. L. Zhang, Z. Zhou, S. Zhou, *Polym. Chem.* **2016**, *7*, 515–518.

14 Y. Hong, J. W. Y. Lam, B. Z. Tang, *Chem. Commun.* **2009**, *29*, 4332–4353.

15 A. Qin, J. W. Y. Lam, B. Z. Tang, *Prog. Polym. Sci.* **2012**, *37*, 182–209.

16 S. Chen, Z. Qin, T. Liu, X. Wu, Y. Li, H. Li, Y. Song, Y. Li, *Phys. Chem. Chem. Phys.* **2013**, *15*, 12660–12666.

17 (a) R. Deans, J. Kim, M. R. Machacek, T. M. Swager, *J. Am. Chem. Soc.* **2000**, *122*, 8565–8566; (b) B. C. Englert, M. D. Smith, K. I. Hardcastle, U. H. F. Bunz, *Macromolecules* **2004**, *37*, 8212–8221; (c) D. Zhao, T. M. Swager, *Org. Lett.* **2005**, *7*, 4357–4360; (d) C. H. Zhao, A. Wakamiya, S. Yamaguchi, *Macromolecules* **2007**, *40*, 3898–3900; (e) A. Wakamiya, K. Mori, S. Yamaguchi, *Angew. Chem. Int. Ed.* **2007**, *46*, 4273–4276.

18 A. D. Cuedias, M. Urien, S. Lecommandoux, G. Wantz, E. Cloutet, H. Cramail, *Org. Electron.* **2006**, *7*, 576–578.

19 C. Yang, H. S. Song, D. Liu, *J. Mater. Sci.* **2012**, *47*, 3315–3319.

20 (a) N. A. Rice, A. Adronoc, *Macromolecules* **2013**, *46*, 3850–3860; (b) A. Elscher, S. Kirchmeyer, W. Ovenich, U. Merker, K. Reuter, PEDOT: Principle and Applications of an Intrinsically Conductive polymer; CRC Press, Taylor and Francis Group, **2010**; (c) K. Takagi, E. Kawagita, R. Kouchi, J. Polym. Sci. A Polym. Chem. **2014**, *52*, 2166–2174.

21 J. Lee, H. J. Cho, N. S. Cho, D. H. Hwing, J. M. Kang, E. Lim, J. I. Lee, H. K. Shim, *J. Polym. Sci. A Polym. Chem.* **2005**, *44*, 2943–2954.

22 B. B. Carbas, A. Kivrak, A. M. Onal, *Electrochim. Acta.* **2011**, *58*, 223–230.

23 Q. Jiang, S. Zhen, D. Mo, K. Lin, S. Ming, Z. Wang, C. Liu, J. Xu, Y. Yao, X. Duan, D. Zhu, H. Shi, *J. Polym. Sci. A Polym. Chem.* **2016**, *54*, 325–334.

24 R. Wang, W. Z. Wang, G. Z. Yang, T. Liu, J. Yu, Y. Jiang, *J. Polym. Sci. A Polym. Chem.* **2008**, *46*, 790–802.

25 D. J. Liaw, K. L. Wang, E. T. Kang, S. P. Pujari, M. H. Chen, Y. C. Huang, B. C. Tao, K. R. Lee, J. Y. Lai, *J. Polym. Sci. A Polym. Chem.* **2007**, *47*, 991–1002.

26 Q. Peng, M. Li, S. Lu, X. Tang, *Macromol. Rapid Commun.* **2007**, *28*, 785–791.

27 J. Oriou, F. Ng, G. Hadziioannou, C. Brochon, E. Cloutet, *J. Polym. Sci. A Polym. Chem.* **2015**, *53*, 2059–2068.

28 J. Shi, Y. Wu, S. Sun, B. Tong, J. Zhi, Y. Dong, *J. Polym. Sci. A Polym. Chem.* **2013**, *51*, 229–240.

29 W. B. Jia, H. W. Wang, L. M. Yang, H. b. Lu, L. Kong, Y. P. Tian, X. T. Tao, J. X. Yang, *J. Mater. Chem. C* **2013**, *1*, 7092–7101.

30 M. A. Nair, S. Patil, *J. Polym. Sci. A Polym. Chem.* **2013**, *51*, 4241–4260.

31 K. Zhang, New Conjugated Polymers Based on Benzodifuranone and Diketopyrrolopurrole; Disserta Verlag, **2012**.

32 E. Ramachandran, R. Dhamodharan, *J. Mater. Chem. C* **2015**, *3*, 8642–8648.

33 X. Y. Shun, Y. J. Wang, E. Zhao, W. Z. Yuan, Y. Liu, P. Lu, A. Qin, Y. Ma, J. Z. Sun, B. Z. Tang, *J. Phys. Chem. C* **2013**, *117*, 7334–7347.

34 R. Hu, N. L. C. Leung, B. Z. Tang, *Chem. Soc. Rev.* **2014**, *43*, 4494–4562.

35 Y. Liu, Y. Zhang, Q. Lan, Z. Qin, S. liu, C. Zhao, Z. Chi, J. Xu, *J. Polym. Sci. A Polym. Chem.* **2013**, *51*, 1302–1314.

36 (a) L. Wang, Z. Zheng, Z. Yu, J. Zheng, M. Fang, J. Wu, Y. Tian, H. Zhou, *J. Mater. Chem. C* **2013**, *1*, 6952–6959; (b) L. Wang, Y. Shen, Q. Zhu, W. Xu, M. Yang, H. Zhou, J. Wu, Y. Tian, *J. Phys. Chem. C* **2014**, *118*, 8531–8540.

37 Y. Zhou, P. Peng, L. Han, W. Tian, *Synth. Met.* **2007**, *157*, 502–507.